

Theory of photoinduced ferromagnetism in dilute magnetic semiconductors

Subodha Mishra, Gouri Shankar Tripathi,* and Sashi Satpathy

Department of Physics and Astronomy, University of Missouri, Columbia, Missouri 65211, USA

(Received 10 August 2007; revised manuscript received 13 November 2007; published 26 March 2008)

We study the photoinduced ferromagnetism in the dilute magnetic semiconductors by solving a Hamiltonian model that consists of localized magnetic moments interacting with the photoexcited itinerant carriers. The spin states of the itinerant carriers are split due to the interaction with the localized magnetic moments, which are assumed to be in thermal equilibrium in the local magnetic field due to the carriers. The time dependence of the light-matter interaction term is eliminated by a unitary transformation and the resulting Hamiltonian is solved by making a Bogoliubov-Valatin transformation or by a variational approach using a Bardeen-Cooper-Schrieffer-type wave function. Without incident light, there are no carriers present to mediate magnetic interaction between the localized spins, so that the system is nonmagnetic. When light is present, the photoexcited carriers mediate a ferromagnetic interaction between the localized moments resulting in a ferromagnetic state, with a transition to a paramagnetic state as temperature is increased beyond T_c . The magnitude of T_c is determined by the parameters of the system such as the strength of the light-matter coupling, the frequency of light, interaction strength of the carriers with the localized moments, etc. Even for a sub-band-gap light frequency, there are induced carriers, primarily due to the Rabi oscillations, leading to a small but nonzero T_c . We find that for typical parameters, T_c is about a fraction of a Kelvin or so, which is sizable. In systems which are already ferromagnetic such as GaAs(Mn), the incident light would enhance the T_c by this amount, an effect which has been recently observed.

DOI: [10.1103/PhysRevB.77.125216](https://doi.org/10.1103/PhysRevB.77.125216)

PACS number(s): 75.50.Pp, 78.20.Jq, 78.30.Fs

I. INTRODUCTION

The interplay between light and magnetization is well known since the discovery of the Faraday and the Kerr effects.¹ However, it is only recently that a great deal of attention has been focused on the photoinduced magnetization, where ferromagnetism is induced or enhanced by the interaction with the incident light. The subject has acquired added importance in view of the search for materials with spin-polarized electrons to be relevant in the emerging area of spintronics.²

Photoinduced magnetization was first demonstrated by Krenn *et al.*³ who found a magnetization signal in $\text{Hg}_{1-x}\text{Mn}_x\text{Te}$ which depends characteristically on the degree of polarization of the exciting radiation. Later on, Awschalom *et al.*⁴ extended this method to the observation of time resolved phenomena in the photoinduced magnetization of $\text{Cd}_{1-x}\text{Mn}_x\text{Te}$. Since then, the effect has been extensively studied in a variety of systems including diluted magnetic semiconductors and their quantum wells,⁵ cyanometalate based magnets,^{6,7} spin crossover complexes,⁸ doped manganites,⁹ spinel ferrite films,¹⁰ and organic based magnets.¹¹

A number of early experiments regarding the photoinduced magnetization have been reported for the semiconductor systems. Kosihara *et al.*⁵ observed a ferromagnetic order by photogenerated carriers in the heterostructure (In,Mn)As/GaSb. At low temperatures, samples preserved the ferromagnetic order even after light is switched off. They attribute the effect to hole transfer from GaSb to InMnAs in the heterostructure, which enhances a ferromagnetic spin exchange among Mn ions in the InMnAs layer. On the other hand, Oiwa *et al.*¹² reported photoinduced magnetization in ferromagnetic (Ga,Mn)As thin films caused by spin-

polarized holes generated optically. The observed results suggest that a small amount of nonequilibrium carrier spins can cause collective rotation of Mn spins presumably through p - d exchange interaction. Mitsumori *et al.*¹³ observed the occurrence of very fast photoinduced magnetization rotation and its relaxation in the picosecond time scale in the ferromagnetic (Ga,Mn)As epilayers. While rotation occurs instantaneously with generation of hole spins, relaxation takes place within some tens of picoseconds resulting from strong damping. Very recently, photomagnetism has been observed in GaAs(Mn), where a transient increase of T_c by about 0.5 K has been observed with laser irradiation.¹⁴

While there has been a considerable amount of experimental work, only recently have the theorists begun investigating the problem. Piermarocchi *et al.*¹⁵ have reported a mechanism of coupling of spins localized in neighboring quantum dots by virtual excitation of delocalized exciton states in the host material by a light field. This indirect exchange interaction termed as the optical RKKY interaction is analogous to the RKKY interaction; the difference from the usual one is that the carriers mediating the magnetic interaction are produced by the external light. Quite recently, the photoinduced ferromagnetism was theoretically studied in the dilute magnetic semiconductors by Fernandez-Rossier *et al.*¹⁶ with special emphasis on magnetization induced by the sub-band-gap radiation. In this paper, our emphasis is not particularly on the sub-band-gap radiation, rather for the case where the photon energy is appreciably above the semiconductor band gap (an eV or so), so that a relatively large number of carriers are photoexcited. We study the photoinduced magnetization by solving a model Hamiltonian within a mean-field approach by constructing a Bardeen-Cooper-Schrieffer-type wave function¹⁷ or, equivalently, making a Bogoliubov-Valatin transformation.^{18,19} The predicted transi-

tion temperature T_c can be as large as a fraction of a Kelvin or so for typical parameters.

II. HAMILTONIAN AND UNITARY TRANSFORMATION

We consider isotropic conduction and valence bands for the electrons and holes, which are spin split through an exchange interaction with the magnetic ions. Our model Hamiltonian consists of the one-particle energies for the electron and the holes, the Coulomb interaction, plus the coupling of the carriers to the light field, treated as classical. The Hamiltonian \mathcal{H} is thus written as the sum of these three terms,

$$\mathcal{H} = \mathcal{H}_{kin} + \mathcal{H}_c + \mathcal{H}_L(t). \quad (1)$$

The kinetic energy term is given by

$$\mathcal{H}_{kin} = \sum_{k\sigma} (E_{k\sigma}^e c_{k\sigma}^\dagger c_{k\sigma} + E_{k\sigma}^h d_{k\sigma}^\dagger d_{k\sigma}), \quad (2)$$

where $c_{k\sigma}^\dagger, c_{k\sigma}$ and $d_{k\sigma}^\dagger, d_{k\sigma}$ are the field operators for the electrons and holes, respectively. The single-particle energies are given by the expressions

$$E_{k\sigma}^e = E_g + \frac{\hbar^2 k^2}{2m_e} \mp \eta_e \langle M \rangle \quad (3)$$

and

$$E_{k\sigma}^h = \frac{\hbar^2 k^2}{2m_h} \mp \eta_h \langle M \rangle, \quad (4)$$

which include the Zeeman splitting due to the electron interaction with the localized spins. For the sake of concreteness, we take the localized spins as manganese spins ($S=5/2$) as is relevant for many dilute magnetic semiconductors. The localized spins occur randomly in the solid and there is no direct interaction between them. In the above equations, \mp describes the Zeeman splitting of the up-spin and the down-spin states with $\eta_e = J_e c / (g\mu_B)$ and $\eta_h = J_h c / (g\mu_B)$, where J_e and J_h are the electron and hole exchange interactions with the localized Mn moments, $\langle M \rangle = g\mu_B \langle S \rangle$ is the average moment of a Mn atom, concentration c is the number of Mn atoms per unit volume, m_e and m_h are the electron and hole masses, respectively, and E_g is the band gap.

The Coulomb interaction part consists of three terms, $\mathcal{H}_c = \mathcal{H}_{ee} + \mathcal{H}_{hh} + \mathcal{H}_{eh}$, where the electron-electron interaction term is

$$\mathcal{H}_{ee} = \frac{1}{2} \sum_{kk'q\sigma\sigma'} V_q c_{k+q,\sigma}^\dagger c_{k'-q,\sigma'}^\dagger c_{k'\sigma'} c_{k\sigma}, \quad (5)$$

with a similar term for the hole-hole interaction, while the electron-hole interaction is given by the expression

$$\mathcal{H}_{eh} = - \sum_{kk'q\sigma\sigma'} V_q c_{k+q,\sigma}^\dagger d_{k'-q,\sigma'}^\dagger d_{k'\sigma'} c_{k\sigma}. \quad (6)$$

The final term is the coupling to the external electromagnetic field of frequency ω , which in the ‘‘rotating wave approximation’’ is given by

$$\mathcal{H}_L(t) = \lambda \sum_k \rho_k [(c_{k\uparrow}^\dagger d_{-k\downarrow}^\dagger + c_{k\downarrow}^\dagger d_{-k\uparrow}^\dagger) e^{-i\omega t} + \text{H.c.}], \quad (7)$$

where $\lambda\rho_k$ is the coupling strength for the creation of the electron-hole pair with momentum k . In the usual dipole approximation, it is proportional to the matrix element of the momentum operator between the conduction and the valence band wave functions and has the form²⁰⁻²²

$$\lambda\rho_k = eE \langle \psi_{v,k} | \hat{e} \cdot \vec{p} | \psi_{c,k} \rangle / m\omega, \quad (8)$$

where E is the strength of the electric field and \hat{e} is the electric polarization vector. The matrix element may be computed once the wave functions are known, but here, for simplicity, we neglect the momentum dependence of the matrix elements, so that $\rho_k = 1$ and thus the parameter λ indicates the strength of the interaction. Figure 1 illustrates the basic mechanism of the photoinduced magnetization discussed in the paper.

The time dependence of Eq. (7) can be eliminated by an appropriate unitary transformation, as is well known from the Rabi problem, viz., $|\tilde{\Psi}(t)\rangle = e^{-iS} |\Psi(t)\rangle$, so that the transformed Hamiltonian $\tilde{\mathcal{H}}$ that describes the time evolution of the system via the Schrödinger equation, $i\hbar \partial \tilde{\Psi}(t) / \partial t = \tilde{\mathcal{H}} \tilde{\Psi}(t)$, is given by

$$\tilde{\mathcal{H}} = e^{-iS} \mathcal{H} e^{iS} + i\hbar \left(\frac{\partial}{\partial t} e^{-iS} \right) e^{iS}. \quad (9)$$

Taking the Hermitian matrix S to be

$$S = - \frac{\omega t}{2} \sum_{k\sigma} (c_{k\sigma}^\dagger c_{k\sigma} + d_{k\sigma}^\dagger d_{k\sigma}), \quad (10)$$

the Hamiltonian becomes

$$\begin{aligned} \tilde{\mathcal{H}} = & \sum_{k\sigma} (E_{k\sigma}^e - \hbar\omega/2) c_{k\sigma}^\dagger c_{k\sigma} + (E_{k\sigma}^h - \hbar\omega/2) d_{k\sigma}^\dagger d_{k\sigma} \\ & + \lambda \sum_k \{ \rho_k (c_{k\uparrow}^\dagger d_{-k\downarrow}^\dagger + c_{k\downarrow}^\dagger d_{-k\uparrow}^\dagger) + \text{H.c.} \} + \mathcal{H}_c. \end{aligned} \quad (11)$$

This is a direct extension of the transformation of Comte and Mahler for the nonmagnetic case^{22,24} and has been also used by Fernandez-Rossier *et al.*¹⁶ in their work.

Thus, the time has been eliminated in the transformed Hamiltonian [Eq. (11)], which may be interpreted as a ‘‘quasi-free-energy’’ with the chemical potential for the creation of an electron-hole pair given by $\mu = \hbar\omega$. One can thus write the transformed Hamiltonian in the form $\tilde{\mathcal{H}} = \mathcal{H}_{QE} - \mu N$, where the total number of electrons $N = \sum_{k\sigma} c_{k\sigma}^\dagger c_{k\sigma}$ is also equal to the number of electron-hole pairs since the optically accessible states contain an equal number of electrons and holes. It is convenient to define a scaled chemical potential μ' by measuring the photon energy with respect to the band gap, so that

$$\mu' = \hbar\omega - E_g. \quad (12)$$

III. BARDEEN-COOPER-SCHRIEFFER WAVE FUNCTION

In this section, we calculate the free energy of the system using an approach similar to the BCS solution in the theory of superconductivity. While in the BCS theory, the wave function is written as a coherent superposition of the Cooper pairs with zero net momentum and spin; in the present case, the variational wave function is a superposition of the electron-hole pairs, again of zero momentum and spin, generated by the coupling to light. We construct the variational ground-state wave function for our system as

$$|\Psi\rangle = \prod_{k\sigma} (u_{k\sigma} + v_{k\sigma} c_{k\sigma}^\dagger d_{-k-\sigma}^\dagger) |0\rangle, \quad (13)$$

where $|0\rangle$ is the intrinsic vacuum state for the semiconductor (filled valence and empty conduction bands). $v_{k\sigma}$ is the probability amplitude for the creation of an electron-hole pair with the electron momentum and spin of $k\sigma$ and a hole with the opposite momentum and spin, while $u_{k\sigma}$ is the probability amplitude for the absence of such pair excitation. The normalization condition is, as usual,

$$u_{k\sigma}^2 + v_{k\sigma}^2 = 1, \quad (14)$$

and the coefficients $u_{k\sigma}$ and $v_{k\sigma}$ may be chosen as real.

For the simplicity of notation, throughout this paper, we use the unbarred quantities as referring to the electron-hole pairs with a spin \uparrow electron and a spin \downarrow hole (and the barred quantities as referring to a spin \downarrow electron and a spin \uparrow hole), so that the probability amplitudes appearing in the BCS wave function are written as

$$\begin{aligned} u_k &\equiv u_{k\uparrow}, & v_k &\equiv v_{k\downarrow}, \\ \bar{u}_k &\equiv u_{k\downarrow}, & \bar{v}_k &\equiv v_{k\uparrow}. \end{aligned} \quad (15)$$

The BCS wave function [Eq. (13)] is a generalization of a similar treatment of the photoexcited electron-hole pairs by earlier authors, who have used it to describe the (Bose condensed) excitons in the dilute limit and Cooper-type pairs in the dense limit.^{22,24-26} In the present case, the localized moments of the magnetic impurities break the symmetry between the spin-up and spin-down electrons, so that the barred and the unbarred quantities such as the amplitudes u_k and \bar{u}_k are different. Since the strength of the exchange interaction with the localized moments is different for the electrons and the holes, the presence of the electron-hole pairs affects the magnetism of the localized moments, even though there is no net magnetization for the carriers. The localized magnetic moments, in turn, affect the energies of the electrons and the holes through the Zeeman term, so that all quantities have to be determined self-consistently (Fig. 1).

We now calculate the expectation value of the ‘‘free energy’’ from Eq. (11) to get

$$\begin{aligned} F_0 = \langle \Psi | \tilde{\mathcal{H}} | \Psi \rangle &= \sum_k (\xi_k^+ v_k^2 + \xi_k^- \bar{v}_k^2) - \sum_{kk'} V_{k-k'} (u_k v_k u_{k'} v_{k'} \\ &+ \bar{u}_k \bar{v}_k \bar{u}_{k'} \bar{v}_{k'} + v_k^2 v_k^2 + \bar{v}_k^2 \bar{v}_k^2) - 2 \sum_k \lambda \rho_k (u_k v_k + \bar{u}_k \bar{v}_k). \end{aligned} \quad (16)$$

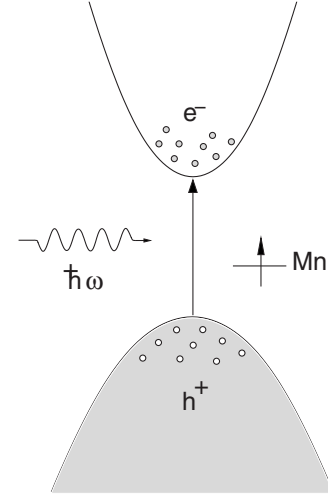


FIG. 1. A schematic picture of the photoinduced ferromagnetism in the dilute magnetic semiconductors. The electrons and holes created by the incident light mediate the magnetic interaction between the localized Mn moments, resulting in a ferromagnetic state below a critical temperature T_c .

Now, using the normalization conditions given by Eq. (14) and minimizing the energy with respect to v_k and \bar{v}_k , so that $\partial F_0 / \partial v_k = 0$ and $\partial F_0 / \partial \bar{v}_k = 0$, we get the two conditions, the solution of which will give us the occupation amplitudes u_k , v_k , \bar{u}_k , and \bar{v}_k , viz.,

$$\begin{aligned} \frac{1}{2} \Delta_k (u_k^2 - v_k^2) - u_k v_k (\xi_k^+ + \Omega_k) &= 0, \\ \frac{1}{2} \bar{\Delta}_k (\bar{u}_k^2 - \bar{v}_k^2) - \bar{u}_k \bar{v}_k (\xi_k^- + \bar{\Omega}_k) &= 0. \end{aligned} \quad (17)$$

Here, ξ_k^+ is the energy of the electron-hole pair excitation with a spin-up electron and a spin-down hole measured with respect to the photon energy

$$\xi_k^+ = E_{k\uparrow}^e + E_{k\downarrow}^h - \hbar\omega \quad (18)$$

and, similarly,

$$\xi_k^- = E_{k\downarrow}^e + E_{k\uparrow}^h - \hbar\omega, \quad (19)$$

so that from Eqs. (3) and (4), we have

$$\xi_k^\pm = E_g + \frac{\hbar^2 k^2}{2m^*} \mp \eta \langle M \rangle - \hbar\omega, \quad (20)$$

where $\eta = \eta_e - \eta_h = Jc / (g\mu_B)$, $J = J_e - J_h$, and the effective mass of the electron-hole pair $m^{*-1} = m_e^{-1} + m_h^{-1}$. The electron-hole pair excitation energies are sketched in Fig. 2. The other quantities appearing in the equations of Eq. (17) above are defined as

$$\Delta_k = 2 \sum_{k'} V_{k-k'} u_k v_{k'} + 2\lambda \rho_k,$$

$$\bar{\Delta}_k = 2 \sum_{k'} V_{k-k'} \bar{u}_k \bar{v}_{k'} + 2\lambda \rho_k,$$

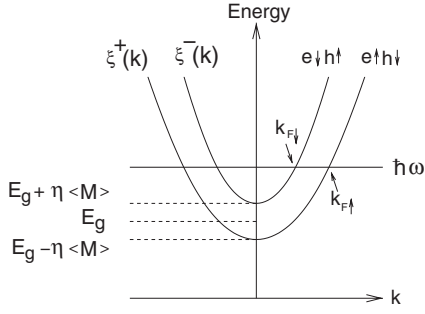


FIG. 2. Energy of the electron-hole pairs of two different spin types produced by photoexcitation. ξ^\pm are the two-particle energies measured with respect to the chemical potential $\hbar\omega$ [see Eq. (20)].

$$\begin{aligned}\Omega_k &= -2 \sum_{k'} V_{k-k'} v_{k'}^2, \\ \bar{\Omega}_k &= -2 \sum_{k'} V_{k-k'} \bar{v}_{k'}^2.\end{aligned}\quad (21)$$

We need to solve for the occupation amplitudes u_k , v_k , \bar{u}_k , and \bar{v}_k self-consistently from these equations, which are taken up in the later part of the next section. We note that in the case of no interaction ($V=0$ and $\lambda=0$), the BCS free energy [Eq. (16)] boils down to the energy of the noninteracting system with the electron-hole pair states occupied up to the chemical potential (i.e., v_k^2 and \bar{v}_k^2 equal to 1 below $\hbar\omega$ and 0 above).

IV. BOGOLIUBOV-VALATIN TRANSFORMATION

Analogous to the BCS Hamiltonian in the theory of superconductivity, the Hamiltonian [Eq. (11)] may be diagonalized using the Bogoliubov-Valatin transformations, which in addition would yield the excitation energies. Toward this end, we define new fermion operators as follows:

$$\begin{aligned}\alpha_{k\sigma}^\dagger &= u_{k\sigma} c_{k\sigma}^\dagger + v_{k\sigma} d_{-k-\sigma}, \\ \beta_{k\sigma}^\dagger &= u_{k\sigma} d_{k-\sigma}^\dagger - v_{k\sigma} c_{-k\sigma},\end{aligned}\quad (22)$$

with the normalization condition [Eq. (14)]. The inverse transformation is given by

$$\begin{aligned}c_{k\sigma} &= u_{k\sigma} \alpha_{k\sigma} - v_{k\sigma} \beta_{-k\sigma}^\dagger, \\ d_{k\sigma} &= u_{k-\sigma} \beta_{k-\sigma} + v_{k-\sigma} \alpha_{-k-\sigma}^\dagger.\end{aligned}\quad (23)$$

The occupation amplitudes are indicated in Fig. 3 for the spin-up pair (spin-up electron and spin-down hole) for typical Hamiltonian parameters. Without any interactions, the pair states are occupied up to the Fermi momentum $k_{F\uparrow}$ or $k_{F\downarrow}$ for the spin-up pair and the spin-down pair, respectively, such that

$$\frac{\hbar^2 k_{F\uparrow(\downarrow)}^2}{2m^*} \mp \eta \langle M \rangle = \hbar\omega - E_g, \quad (24)$$

while the interactions smear out the occupation amplitudes around the Fermi energy. The quasiparticle operators $\alpha_{k\sigma}^\dagger$ are

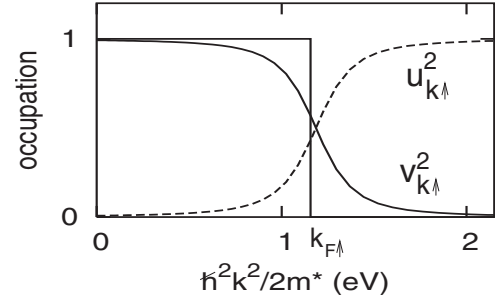


FIG. 3. Electron-hole pair amplitudes $u_{k\uparrow}$ and $v_{k\uparrow}$ as a function of momentum k . Pairs of spin-up electrons and spin-down holes are filled up to the Fermi momentum $k_{F\uparrow}$ without any interactions. The step function describes $v_{k\uparrow}^2$ for the case with zero interactions ($\lambda = V_0 = 0$), while both the Coulomb interaction and the coupling to light smear out the Fermi surface. Here, the parameters are $\lambda = 0.1$ eV, $m^* = 0.1m_e$, $V_0 = 100$ eV \AA^3 , and $\hbar\omega - E_g = 1$ eV. The pair amplitudes for the other spin type, $u_{k\downarrow}$ and $v_{k\downarrow}$, are slightly shifted to the left since $k_{F\downarrow}$ is slightly lower than $k_{F\uparrow}$ because of the spin splitting term, as seen from Eq. (24).

electronlike for the pair-excitation energy larger than $\hbar\omega$ and are holelike for lower energies, while the quasiparticles $\beta_{k\sigma}^\dagger$ are opposite in character. One can easily show by direct evaluation that the BCS state $|\Psi\rangle$ plays the role of vacuum for the Bogoliubov quasiparticles $\alpha_{k\sigma}^\dagger$ and $\beta_{k\sigma}^\dagger$ and the new quasiparticle annihilation operators annihilate the BCS state, so that $\alpha_{k\sigma}|\Psi\rangle = \beta_{k\sigma}|\Psi\rangle = 0$.

With the above transformation and neglecting the products of four Bogoliubov operators (which give higher order corrections), the free energy operator [Eq. (11)] becomes

$$\begin{aligned}F_T &= F_0 + \sum_{k\sigma} (E_{k\sigma}^e - \hbar\omega/2 + A_{k\sigma}) \alpha_{k\sigma}^\dagger \alpha_{k\sigma} + (E_{k-\sigma}^h - \hbar\omega/2 \\ &+ A_{k\sigma}) \beta_{k\sigma}^\dagger \beta_{k\sigma} + B_{k\sigma} (\alpha_{k\sigma}^\dagger \beta_{-k\sigma}^\dagger + \beta_{-k\sigma} \alpha_{k\sigma}),\end{aligned}\quad (25)$$

where the first term F_0 is the BCS free energy [Eq. (16)]. In the above equation,

$$\begin{aligned}A_{k\uparrow} &\equiv A_k = \left\{ \frac{1}{2} \Omega_k - (\xi_k^+ + \Omega_k) v_k^2 + \Delta_k u_k v_k \right\}, \\ B_{k\uparrow} &\equiv B_k = \left\{ \frac{1}{2} \Delta_k (u_k^2 - v_k^2) - u_k v_k (\xi_k^+ + \Omega_k) \right\},\end{aligned}\quad (26)$$

and $A_{k\downarrow} \equiv \bar{A}_k$ and $\bar{B}_{k\downarrow} \equiv \bar{B}_k$ are defined by replacing ξ_k^+ by ξ_k^- and all unbarred quantities by the barred quantities in the expressions [Eq. (26)].

The free energy operator [Eq. (25)] becomes diagonalized by choosing $B_{k\sigma} = 0$, which yields the two equations [Eq. (17)] we have already obtained. Solving these two equations along with the normalization condition [Eq. (14)], we get

$$\begin{aligned}u_k^2 &= \frac{1}{2} \left[1 + \frac{\xi_k^+ + \Omega_k}{\sqrt{\Delta_k^2 + (\xi_k^+ + \Omega_k)^2}} \right], \\ v_k^2 &= \frac{1}{2} \left[1 - \frac{\xi_k^+ + \Omega_k}{\sqrt{\Delta_k^2 + (\xi_k^+ + \Omega_k)^2}} \right],\end{aligned}\quad (27)$$

and similar expressions for \bar{u}_k^2 and \bar{v}_k^2 by replacing ξ_k^+ by ξ_k^- and the unbarred quantities with the barred quantities in Eq.

(27). These equations together with Eq. (21) form the set of transcendental equations, which have to be solved iteratively. The solution then provides the ground-state wave function and energy F_0 , which can be evaluated using the BCS expression [Eq. (16)], as well as the quasiparticle excitation energies for the particles and the holes from the Bogoliubov-Valatin expression [Eq. (25)]. The typical pair-occupation amplitudes u_k and v_k have been shown in Fig. 2. By combining Eqs. (27) and (21), we get the gap equation

$$\Delta_k = 2\lambda\rho_k + \sum_{k'} V_{kk'} \frac{\Delta_{k'}}{\sqrt{\Delta_{k'}^2 + (\xi_{k'}^+ + \Omega_{k'})^2}} \quad (28)$$

and a similar equation for $\bar{\Delta}_k$.

The ground-state energy [Eq. (16)] may be rewritten in terms of the gap parameter to yield

$$F_0 = \sum_k [(\xi_k^+ + \Omega_k/2)v_k^2 + (\xi_k^- + \bar{\Omega}_k/2)\bar{v}_k^2 - (\Delta_k u_k v_k + \bar{\Delta}_k \bar{u}_k \bar{v}_k)/2 - \lambda\rho_k(u_k v_k + \bar{u}_k \bar{v}_k)]. \quad (29)$$

While the Bogoliubov-Valatin expression [Eq. (25)] yields the energy of the individual electron and hole quasiparticles, in our problem, the relevant excitations are the electron-hole pair excitations defined by $(\alpha_{k\sigma}^\dagger, \beta_{k\sigma}^\dagger)$, where the momentum and spin are conserved. It is straightforward to show from the Bogoliubov-Valatin expression that the energy of the pair excitation is given by

$$E_{k\uparrow} = \sqrt{\Delta_k^2 + (\xi_k^+ + \Omega_k)^2}, \quad (30)$$

for the up-spin electron and down-spin hole $(\alpha_{k\uparrow}^\dagger, \beta_{k\uparrow}^\dagger)$ and a similar expression for the pair with the opposite electron and hole spins, viz., $E_{k\downarrow} = (\bar{\Delta}_k^2 + (\xi_k^- + \bar{\Omega}_k)^2)^{1/2}$.

V. RESULTS AND DISCUSSION

Rabi problem. The present case has considerable similarity with the well-known Rabi problem, for which the time-dependent Schrödinger equation is exactly solvable. In fact, we have already used the transformations [Eq. (10)], which are well known from the solution of the Rabi problem. We briefly state the main results here. Consider a two-level system coupled to light and described by the Hamiltonian

$$\mathcal{H} = \alpha c^\dagger c + \beta d^\dagger d + \lambda(c^\dagger d e^{i\omega t} + d^\dagger c e^{-i\omega t}). \quad (31)$$

If we make a unitary transformation similar to Eq. (10), viz., $S = \omega t c^\dagger c$, then the transformed Hamiltonian becomes $\tilde{\mathcal{H}} = (\alpha + \hbar\omega)c^\dagger c + \beta d^\dagger d + \lambda(c^\dagger d + d^\dagger c)$, so that the energy levels are shifted by the amount $\delta E = 1/2 \times \sqrt{(\Delta E)^2 + 4\lambda^2}$, where the detuning factor ΔE is defined as

$$\Delta E = \hbar(\omega - \omega_{21}), \quad (32)$$

with $\omega_{21} = \beta - \alpha$. If the system starts out at $t=0$ in the lower-energy state $|\alpha\rangle$, then the probability of finding the system at the higher-energy state $|\beta\rangle$ is given by the Rabi expression²³

$$P(t) = \frac{\lambda^2}{\hbar^2 \Omega^2} \sin^2 \Omega t, \quad (33)$$

where the Rabi frequency $\Omega = [\lambda^2/\hbar^2 + (\omega - \omega_{21})^2/4]^{1/2}$. An important point is that although the maximum transition probability occurs for the frequency ω corresponding to the resonance condition $\omega = \omega_{21}$, there is also a nonzero transition probability when the frequency of light is different from the resonance condition. In particular, this allows for the possibility of photoinduced magnetization even for the sub-band-gap light frequency.^{16,27}

Interaction parameters. We have in mind the typical semiconductor systems such as GaAs(Mn), ZnS(Mn), etc. The Coulomb interaction term appearing in the Hamiltonian [Eqs. (5) and (6)] is given by $V_q = 4\pi e^2/(\epsilon q^2)$, but in our discussions below, we replace it, for the sake of simplicity, by a contact interaction term $V(\vec{r}) = V_0 \delta(\vec{r})$ without changing the qualitative physics. With the box normalization with the box volume \mathcal{V} , this leads to the momentum-independent interaction $V_q = V_0/\mathcal{V}$. The magnitude of the contact interaction may be estimated by requiring that it produces the exciton binding energy ($\text{BE} \approx V_0 |\psi_{ex}(0)|^2$) for typical semiconductors ($\epsilon \approx 10$, $m^* \approx 0.5m_e$, and the exciton radius $a_{ex} \approx 10 \text{ \AA}$), so that $V_0 \approx 200 \text{ eV \AA}^3$. Typical values for the other parameters are $J \approx 30 \text{ eV \AA}^3$ (Ref. 16), $m^* \approx 0.1-0.5m_e$, $\lambda \approx 0.1 \text{ eV}$, and Mn concentration $c \approx 2 \times 10^{-3}/\text{\AA}^3$. We note that the magnitude of the parameter λ depends ultimately on the intensity of the laser radiation, as indicated in Eq. (8).

The contact interaction simplifies the gap equation [Eq. (28)], which now reads

$$\Delta = \frac{V_0}{\mathcal{V}} \sum_k \frac{\Delta}{\sqrt{\Delta^2 + (\xi_k^+ + \Omega)^2}} + 2\lambda, \quad (34)$$

where we have taken a momentum-independent light-matter coupling by choosing $\rho_k = 1$. Test calculations show that the basic results are not changed, if a momentum-dependent ρ_k is used instead. A similar equation results for the gap parameter $\bar{\Delta}$ by replacing Δ , Ω , and ξ^+ with $\bar{\Delta}$, $\bar{\Omega}$, and ξ^- , respectively, in Eq. (34). Note that the gap parameters $\Delta, \bar{\Delta}$ as well as the Coulomb terms $\Omega, \bar{\Omega}$ have become independent of k .

To see the effect of the light interaction term, we may set $V_0 = 0$, in which case Eqs. (34) and (21) yield the values $\Delta = 2\lambda$ and $\Omega = 0$, so that the occupation probabilities become

$$v_k^2 = \frac{1}{2} \left[1 - \frac{\xi_k^+}{\sqrt{4\lambda^2 + \xi_k^+}} \right], \quad (35)$$

and similarly for \bar{v}_k^2 . In addition, in the limit of negligible light-matter interaction, $\lambda \rightarrow 0$, we get the simple two-particle picture in the noninteracting limit, so that the electron-hole pair states are filled up to the Fermi momentum corresponding to the energy $\hbar\omega$: $v_k^2 = (1/2)(1 - \xi_k^+ / |\xi_k^+|) = \theta(\hbar\omega - E_{k\uparrow}^e - E_{k\downarrow}^h)$ with a similar expression holding for \bar{v}_k^2 , where θ is the step function. For the case with finite interactions, the gap equation has to be solved self-consistently.

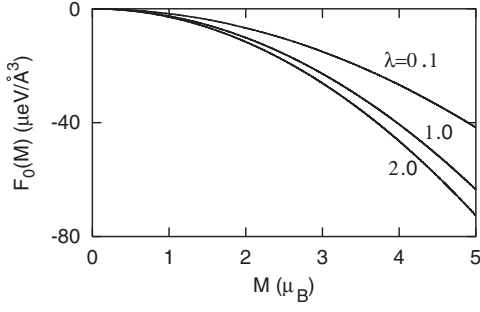


FIG. 4. Free energy F_0 computed using Eq. (29) as a function of magnetic moment M for different values of the coupling parameter λ (in units of eV). Energy is measured with respect to $F_0(M=0)$. The parameters are $V_0=200$ eV \AA^3 , $\mu'=\hbar\omega-E_g=1$ eV, and $m^*=0.4m_e$.

The typical occupation probabilities u_k^2, v_k^2 have been shown in Fig. 3 for typical parameters. In Figs. 4 and 5, we plot the free energy of the system as a function of the magnetic moment for different values of the interaction parameter λ and the chemical potential keeping the other parameters fixed. The free energy decreases as a function of the average Mn magnetic moment, as there is an increased net gain of the Zeeman energy for the electron-hole pairs with increasing magnetization M . As the chemical potential is increased, the Fermi surface swells and a larger number of electron-hole pairs are created, which results in a stronger change of the free energy as a function of the magnetization (Fig. 5).

Temperature dependence of magnetization. We calculate the magnetization of the Mn moments in the spirit of the mean-field approximation. Each Mn moment experiences an effective magnetic field H_{eff} given by

$$H_{eff} = -\frac{\partial F_0(M)}{\partial M}, \quad (36)$$

so that the magnetization is

$$M(T) = g\mu_B \sum_{S=-5/2}^{+5/2} S e^{-\beta H_{eff}(M)S} / Z, \quad (37)$$

where the partition function $Z = \sum_{S=-5/2}^{+5/2} e^{-\beta H_{eff}(M)S}$, $\beta = (k_B T)^{-1}$, and $M(S) = g\mu_B S$. The above two equations are solved self-consistently for a given temperature using the

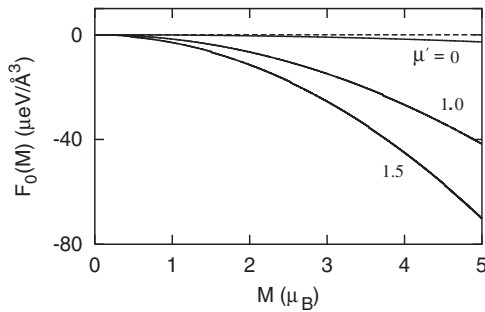


FIG. 5. Same as Fig. 4 for different values of the chemical potential $\mu'=\hbar\omega-E_g$.

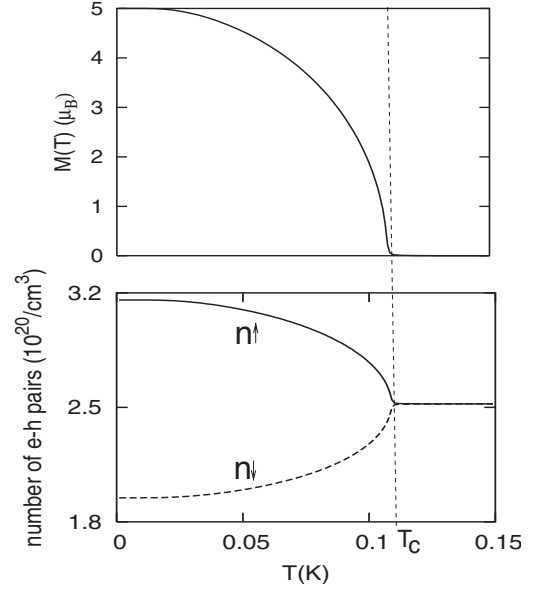


FIG. 6. Dependence of the magnetization M and the number of electron-hole pairs as a function of temperature T . n_\uparrow denotes the number of electron-hole pairs with spin-up electrons and spin-down holes, while n_\downarrow denotes the number of pairs with the opposite spins. Below the critical temperature, n_\uparrow is larger than n_\downarrow because of the lower Zeeman energy of the former pairs, which results in a larger occupancy. The parameters are $V_0=200$ eV \AA^3 , $\mu'=\hbar\omega-E_g=1$ eV, $m^*=0.2m_e$, and $\lambda=0.1$ eV.

free energy expression [Eq. (29)] for calculating the magnetic field.

By expanding the magnetization near T_c and using the free energy expression [Eq. (16)], one can find an analytical expression in the limit of small interaction and large chemical potential, viz., $V_0 \rightarrow 0$, $\lambda \rightarrow 0$, and $\mu' = \hbar\omega - E_g \gg \eta \langle M \rangle$. The expression is

$$k_B T_c = \frac{4}{3} J^2 c^2 \rho(\mu') S(S+1), \quad (38)$$

where $\rho(\mu')$ is the two-particle density of states (electrons and holes) per spin type at the energy corresponding to the chemical potential. For the free-particle parabolic density of states $\rho(\epsilon) \sim \sqrt{\epsilon}$, so that the Fermi-energy density of states may be written as being proportional to the one-third power of the total number of carriers N mediating the magnetic interaction: $\rho(\mu') \sim N^{1/3}$. Such an $N^{1/3}$ dependence seems to be more universal and it has been observed in the intrinsic GaAs(Mn) samples²⁸ without the presence of light, where holes are induced by the Mn dopants.

The calculated temperature dependence of magnetization as well as the carrier densities are shown in Fig. 6, which contains the central result of this paper. A transition is seen from the ferromagnetic to the paramagnetic phase as temperature is increased. For typical parameters, we find the transition temperature T_c to be a fraction of a Kelvin. While the number of the electron-hole pairs is controlled by the chemical potential, the distribution of the pairs between the two different spin types (spin-up electron and spin-down

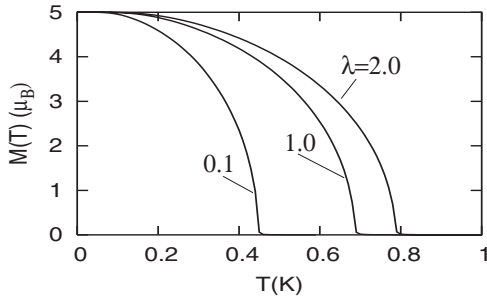


FIG. 7. Magnetization $M(T)$ as a function of temperature T for different values of the light coupling λ (measured in eV). The plot shows a phase transition from paramagnetic to ferromagnetic state as temperature is lowered. A stronger value of λ results in a higher T_c . The parameters are the same as in Fig. 4.

hole or vice versa) is determined by the magnitude of M , which affects the pair energy, as indicated from Fig. 2. The effective magnetic field experienced by the Mn spins is roughly proportional to the difference of the number of the two spin types, as may be seen by keeping the first line in the free energy [Eq. (29)] and using Eqs. (20) and (36), so that $H_{eff} \propto (n_{\uparrow} - n_{\downarrow})$, which in turn implies that this number difference and the magnetization M follow one another, both ultimately going to zero at the transition temperature T_c . In the paramagnetic phase, the photoexcited electron-hole pairs are present, but the number of the two spin types is the same. Obviously, the electron-hole pairs do not contribute to the net magnetic moment of the system as they have zero net spin.

The variation of the magnetic moment M as a function of temperature T for different values of λ and $\hbar\omega$ is shown in Figs. 7 and 8, keeping the other parameters fixed. The observed variation and trends are the same in both the figures, viz., that with the increase in λ and μ , the critical temperature increases. This is due to the fact that with the increase in these quantities, the carrier densities increase, which in turn induce larger magnetization and hence T_c is increased.

In Fig. 9, we show the variation of T_c as a function of the chemical potential. There are two points to notice. The first is that T_c increases with increasing chemical potential, as expected since increasing the chemical potential leads to an

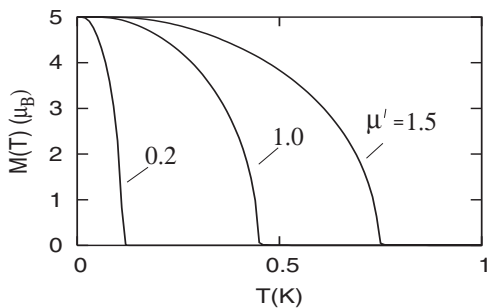


FIG. 8. Magnetization $M(T)$ as a function of temperature T for different values of the chemical potential $\mu' = \hbar\omega - E_g$ for a given value of the light coupling $\lambda = 0.1$ (both quantities are in units of eV). The parameters are the same as in Fig. 7. With increased chemical potential, the number of the photoexcited carriers is increased, which increases T_c .

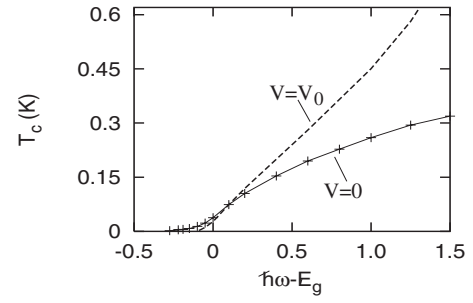


FIG. 9. Critical temperature T_c as a function of the chemical potential $\mu' = \hbar\omega - E_g$. Negative μ' corresponds to sub-band-gap radiation. The parameters are $V_0 = 200 \text{ eV \AA}^3$, $\lambda = 0.1 \text{ eV}$, and $m^* = 0.4m_e$.

increased carrier density, hence to stronger coupling between the magnetic moments. For larger values of the chemical potential the square-root dependence $T_c \propto \rho(\mu') \sim \sqrt{\mu'}$, as predicted by Eq. (38), is more or less followed. The second point is that there is a small magnetization even for $\mu' < 0$, which corresponds to the sub-band-gap radiation. The origin of this effect is easily understood from the Rabi problem, where the system oscillates between the ground-state and the higher-energy state (ground state with no electrons or holes into a state with the electron-hole pairs) even when the radiation is below the resonance frequency. This being the case, the effect is present, even when there is no Coulomb interaction ($V_0 = 0$). In Fig. 9, we have, in fact, taken the Coulomb interaction to be zero, so that the magnetism for the sub-band-gap radiation is entirely due to the Rabi oscillations. With a nonzero V_0 , the figure remains qualitatively the same. We note that the number of carriers excited for a sub-band-gap radiation is small, which results in a relatively small T_c in the sub-band-gap case.

Finally, we study the dependence of T_c on the coupling strength $J = J_e - J_h$ between the electron-hole pairs and the Mn magnetic moments. In Fig. 10, we show a plot of the critical temperature T_c as a function of J^2 . We observe a linear behavior as expected. Since the basic origin of the exchange Hamiltonian goes as $H = J\vec{S} \cdot \vec{s}\delta(r)$, the effective exchange between magnetic moments is $J_{eff} = J^2$ so that $T_c \sim J_{eff} \sim J^2$, as is evident from the expression for T_c [Eq. (38)].

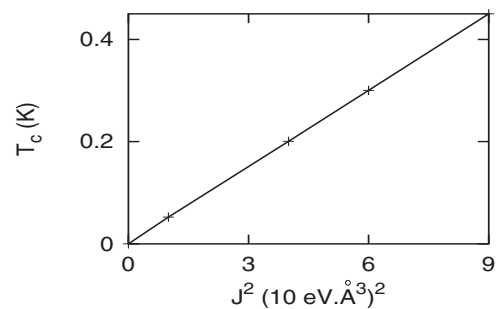


FIG. 10. Critical temperature T_c as a function of $J^2 = (J_e - J_h)^2$, showing a linear dependence in accordance with Eq. (38). Parameters are the same as in Fig. 3 except that $V_0 = 0$ and $\lambda = 0.1 \text{ eV}$.

VI. CONCLUSION

In this paper, we studied the photoinduced magnetization in the dilute magnetic semiconductors by solving in the mean-field approximation a model Hamiltonian which takes into account the Coulomb interaction, light-matter interaction, and the exchange interactions between carriers and the localized magnetic moments. The model assumed no direct interaction between the localized moments and no free carriers without the incident light, so that the system is paramagnetic without the presence of light and can be ferromagnetic only via the indirect interaction with the photoinduced carriers.

The time dependence in the Hamiltonian was eliminated by a unitary transformation and the transformed Hamiltonian was then diagonalized by the Bogoliubov-Valatin transformation or a BCS wave function approach. From the calculated free energy, we computed the magnetization of the system as a function of temperature. There is a para-ferromagnetic transition as temperature is decreased with the transition temperature T_c depending on the various parameters. The radiation frequency is an important parameter.

With increasing frequency, the number of photoexcited electron-hole pairs is increased, which in turn results in a stronger magnetic interaction between the localized moments and a higher value for the T_c . We also observe magnetization even when the photon energy is below the band gap, an effect that is similar to the Rabi oscillations for the sub-band-gap frequencies.

For typical parameters for the dilute magnetic semiconductors, a T_c of a fraction of a Kelvin or so is predicted in the presence of the photoexcited carriers. For the dilute magnetic semiconductors such as GaAs(Mn), where the carriers are already present even without the incident light, the additional carriers photoexcited by the laser radiation should increase the magnitude of T_c , an effect that has just been reported in the literature.¹⁴

ACKNOWLEDGMENTS

This work was supported by the U.S. Air Force Office of Scientific Research under Grant No. AFOSR-FA 9550-05-1-0462.

*Permanent address: Department of Physics, Berhampur University, Berhampur, 760007 Orissa, India.

¹H. J. Zeiger and G. W. Pratt, *Magnetic Interactions in Solids* (Clarendon, Oxford, 1973), p. 440.

²S. Das Sarma, *Am. Sci.* **89**, 516 (2001).

³H. Krenn, W. Zawadzki, and G. Bauer, *Phys. Rev. Lett.* **55**, 1510 (1985).

⁴D. D. Awschalom, J. Warnock, and S. von Molnar, *Phys. Rev. Lett.* **58**, 812 (1987).

⁵S. Koshihara, A. Oiwa, M. Hirasawa, S. Katsumoto, Y. Iye, C. Urano, H. Takagi, and H. Munekata, *Phys. Rev. Lett.* **78**, 4617 (1997).

⁶D. A. Pejakovic, J. L. Manson, J. S. Miller, and A. J. Epstein, *Phys. Rev. Lett.* **85**, 1994 (2000).

⁷T. Kawamoto, Y. Asai, and S. Abe, *Phys. Rev. Lett.* **86**, 348 (2001).

⁸Y. Ogawa, S. Koshihara, K. Koshino, T. Ogawa, C. Urano, and H. Takagi, *Phys. Rev. Lett.* **84**, 3181 (2000).

⁹K. Matsuda, A. Machida, Y. Moritomo, and A. Nakamura, *Phys. Rev. B* **58**, R4203 (1998).

¹⁰Y. Muraoka, H. Tabata, and T. Kawai, *Appl. Phys. Lett.* **77**, 4016 (2000).

¹¹D. A. Pejakovic, C. Kitamura, J. S. Miller, and A. J. Epstein, *Phys. Rev. Lett.* **88**, 057202 (2002).

¹²A. Oiwa, Y. Mitsumori, R. Moriya, T. Slupinski, and H. Munekata, *Phys. Rev. Lett.* **88**, 137202 (2002).

¹³Y. Mitsumori, A. Oiwa, T. Slupinski, H. Maruki, Y. Kashimura,

F. Minami, and H. Munekata, *Phys. Rev. B* **69**, 033203 (2004).

¹⁴J. Wang, I. Cotoros, K. M. Dani, X. Liu, J. K. Furdyna, and D. S. Chemla, *Phys. Rev. Lett.* **98**, 217401 (2007).

¹⁵C. Piermarocchi, P. Chen, L. J. Sham, and D. G. Steel, *Phys. Rev. Lett.* **89**, 167402 (2002).

¹⁶J. Fernandez-Rossier, C. Piermarocchi, P. Chen, A. H. MacDonald, and L. J. Sham, *Phys. Rev. Lett.* **93**, 127201 (2004).

¹⁷J. Bardeen, L. N. Cooper, and J. R. Schrieffer, *Phys. Rev.* **108**, 1175 (1957).

¹⁸N. N. Bogoliubov, *J. Phys. (USSR)* **9**, 23 (1947).

¹⁹J. G. Valatin, *Nuovo Cimento* **7**, 843 (1958).

²⁰F. Bassani and G. Pastori Parravicini, *Electronic States and Optical Transitions in Solids* (Pergamon, New York, 1975).

²¹V. I. Litvinov, K. A. Valuev, and K. D. Tovstyuk, *Sov. Phys. JETP* **55**, 478 (1982).

²²C. Comte and G. Mahler, *Phys. Rev. B* **38**, 10517 (1988).

²³J. J. Sakurai, *Modern Quantum Mechanics* (Addison-Wesley, New York, 1994), p. 320.

²⁴C. Comte and G. Mahler, *Phys. Rev. B* **34**, 7164 (1986).

²⁵Th. Harbich and G. Mahler, *Phys. Status Solidi B* **104**, 185 (1981).

²⁶Th. Harbich and G. Mahler, *Phys. Status Solidi B* **117**, 635 (1983).

²⁷D. Fröhlich, A. Nöthe, and K. Reimann, *Phys. Rev. Lett.* **55**, 1335 (1985).

²⁸A. H. MacDonald, P. Schiffer, and N. Samarth, *Nat. Mater.* **4**, 196 (2005).